Forest Ecology and Management 489 (2021) 119098

Contents lists available at ScienceDirect

Forest Ecology and Management

journal homepage: www.elsevier.com/locate/foreco

The effects of nitrogen addition on soil organic carbon decomposition and microbial C-degradation functional genes abundance in a *Pinus tabulaeformis* forest

Hang Jing [a], Jingjing Li [a,c], Benshuai Yan [b], Furong Wei [a], Guoliang Wang [a,b,*], Guobin Liu [a,b]

[a] State Key Laboratory of Soil Erosion and Dryland Farming on the Loess Plateau, Institute of Soil and Water Conservation, Northwest A&F University, Yangling 712100, Shaanxi Province, China
[b] Institute of Soil and Water Conservation, Chinese Academy of Science and Ministry of Water Resources, Yangling 712100, Shaanxi, China
[c] Upper and Middle Yellow River Bureau, Yellow River Conservancy Commission of the Ministry of Water Resources, Xi'an 710021, Shaanxi, China

ARTICLE INFO

Keywords:
Nitrogen addition
C-cycling functional genes
SOC-degrading enzyme activity
Soil CO_2 emission
Soil organic carbon decomposition

ABSTRACT

Nitrogen (N) deposition affects soil organic carbon (SOC) decomposition, therefore altering the global terrestrial carbon (C) cycle. However, it remains unclear how N deposition affects SOC decomposition by regulating microbial community composition and function, especially C-cycling functional gene composition. We investigated the effects of N addition (0, 3, 6, and 9 g N m^{-2} y^{-1}) on the composition of soil microbial C-cycling functional gene, SOC-degrading enzyme activities, and CO_2 emissions in a *Pinus tabulaeformis* forest. Under low N addition (3 or 6 g N m^{-2} y^{-1}), labile C-degradation gene abundances were significantly increased. Under high N addition (9 g N m^{-2} y^{-1}), C-cycling functional gene abundance and diversity were significantly decreased. These effects were related to the changes in soil NO_3^--N, dissolved organic C, total N, and microbial biomass C contents. Furthermore, low N addition stimulated the activities of SOC-degrading enzyme and CO_2 emissions, whereas high N addition had the inhibitory effect. C-degradation gene abundances were significantly correlated with the SOC-degrading enzyme activities and CO_2 emissions. Increase in CO_2 emission rates were related to the high microbial functional potentials for labile C degradation under low N addition, whereas the lower CO_2 emission rates were related to the low microbial functional potentials for labile as well as recalcitrant C degradation under high N addition. Our study indicated that N deposition may change SOC decomposition by altering the abundance of labile C and recalcitrant C degradation genes.

1. Introduction

Soil organic C (SOC) decomposition impacts on soil C dynamics and the net CO_2 exchange between the atmosphere and biosphere, which have attracted increased attention in the context of global climate change (Riggs and Hobbie, 2016; Xiao et al., 2019). Elevated N deposition has been reported to have the potential to constrain SOC decomposition (Riggs et al., 2015). Microorganisms are the major players in the biogeochemical cycles and are essential to soil ecological functions, especially organic matter decomposition and nutrient cycling (Bardgett et al., 2008; Wang et al., 2019a). However, the response of the functional microbial community to N deposition and how this link to SOC decomposition remain unclear. Understanding the microbe-driven mechanisms for SOC decomposition is of great significance for prediction of ecosystem feedback to climate change.

Anthropogenic N deposition affects soil microbial community by changing soil nutrient contents, pH, plant growth, and plant C allocation belowground in forest ecosystems (Treseder, 2008; Wang et al., 2016b; Zhou et al., 2017). Previous studies have mainly focused on microbial activity and taxonomic composition; the responses of microbial functional traits at the genetic level to N deposition have attracted little attention, and the reported results are inconsistent. For example, Wei et al. (2018) reported a significant increase in C-cycling functional gene abundances at 45 g N m^{-2} once treatment in agricultural ecosystems, whereas Zhang et al. (2017a) reported that 10 g N m^{-2} y^{-1} treatment had no significant effects on functional gene abundances and diversity in

* Corresponding author at: State Key Laboratory of Soil Erosion and Dryland Farming on the Loess Plateau, Institute of Soil and Water Conservation, Northwest A&F University, Yangling 712100, Shaanxi Province, China.
E-mail addresses: hjing@nwsuaf.edu.cn (H. Jing), lijingjing0525@126.com (J. Li), yanbenshuai@126.com (B. Yan), 2929853979@qq.com (F. Wei), glwang@nwsuaf.edu.cn (G. Wang), gbliu@ms.iswc.ac.cn (G. Liu).

https://doi.org/10.1016/j.foreco.2021.119098
Received 16 January 2021; Received in revised form 21 February 2021; Accepted 22 February 2021
Available online 13 March 2021

soil of perennial grass *Bothriochloa ischaemum*, and Eisenlord et al. (2013) observed that 3 g N m^{-2} y^{-1} led to a significant decrease in C-cycling functional gene abundance at sites with low ambient N deposition (~0.4 g N m^{-2} y^{-1}) in hardwood forests of North America. These discrepant findings may be related to the initial N status of the soil, which differs in different ecosystems, and to varying N addition levels (Guo et al., 2017). By sequencing taxonomic marker genes, it was shown that in N-limited ecosystems, low N addition (usually no more than 10 g N m^{-2} y^{-1}) increased microbial biomass and diversity by alleviating the limitation of soil N, decreasing the soil C/N ratio, and promoting plant growth and C inputs from aboveground plant organs (Lv et al., 2017; Zhang et al., 2017a), whereas excessive N addition decreased microbial biomass and diversity by decreasing the allocation of photosynthetic C to the roots by plants or/and inducing soil acidification (Liu et al., 2014; Treseder, 2008). In N-rich tropical forest ecosystems, where soil has higher initial N levels and high soil acidity, N addition generally has only minor effects on plant growth and decreases microbial biomass and diversity mainly by aggravating soil acidification (Wang et al., 2018a; 2018b). Therefore, the effects of N addition on microbial activity and diversity may be related to the changes in soil C and N availability and pH under different amounts of added N. Soil microbial activity and diversity are inherently related to their functional potentials. For example, high abundance of C-cycling genes often indicate the active SOC-degrading enzymes and diverse decomposers (Trivedi et al., 2016; Cheng et al., 2017). Functional gene potentials reflect the abilities of microorganisms involved in biogeochemical processes. Which estimate the microbe-driven mechanisms of SOC decomposition more directly. However, the microbial responses in terms of patterns of C-cycling functional gene abundance to various N addition regimens remain unclear. Further studies concerning this response are needed to enable prediction of functional feedbacks to the climate system and to deepen our understanding of the C cycle.

N deposition is concerned to affect SOC decomposition and soil CO_2 emission by changing microbial biomass and microbial community composition (Edwards et al., 2011; Riggs and Hobbie, 2016; Wang et al., 2015). However, microbial function in biogeochemical processes depends on the activity or behavior associated with their functional genes. Understanding how such microbial functional genes operate within ecological and biogeochemical processes is essential to understanding the mechanisms underlying soil microbe-driven changes in SOC decomposition under N deposition. Trivedi et al. (2016) found a significant positive relationship between SOC-degrading enzyme activities and the abundance of corresponding C-degradation genes, and Cheng et al. (2017) reported that warming enhanced decomposition of old SOC mainly through increasing C-degradation gene abundance. However, various types of C-degradation genes are involved, with targets across the range from labile C (including starch, hemicellulose, pectin, cellulose, and chitin) to recalcitrant C (such as vanillin/lignin and lignin) (Wang et al., 2016a), and these may differentially drive SOC decomposition (Zhang et al., 2017b). For example, Zhou et al. (2011) reported that warming increased soil C release by stimulating genes for degrading labile, but not recalcitrant C. Another study revealed that warming promoted soil organic matter (SOM) decomposition in the surface soil by stimulating either labile or recalcitrant C degradation genes, while in the subsoil of deep samples only recalcitrant C degradation genes were involved (Cheng et al., 2017). It remains unclear how N deposition affects SOC decomposition by means of regulation of various microbial C-degradation functional potentials. In addition, these functional potentials are reported to respond differently depending on the level of added N. Low N addition resulted in higher recalcitrant C degradation gene abundance, but had no influence on levels of those acting on labile C, in a typical semiarid temperate grassland in northern China (Li et al., 2017). High N addition lowered the abundance of both gene types in a hardwood forest ecosystem in North America (Eisenlord et al., 2013). N addition has the various effects on microbial functional genes, but whether resulting in SOC decomposition like other related studies still needs to be verified.

This study aimed to determine how different levels of added N affect microbial C-cycling functional gene community and subsequently influence SOC decomposition. To this end, we conducted a 5-year field experiment in a typical N-restricted, artificial *Pinus tabulaeformis* forest ecosystem on the Loess Plateau in China, in which we measured soil properties, microbial biomass, C-cycling functional gene abundance and composition, and SOC-degrading enzyme activities. In addition, we measured CO_2 emissions to assess SOC decomposition. We hypothesized that (1) in a N-limited ecosystem, low N addition would increase microbial C-cycling functional gene abundances and diversity by increasing soil nutrient contents and enhancing C input from plant litter (leaves and roots) to the soil, whereas high N addition may lead to N saturation, thus reducing the abundance and diversity of these genes; and (2) low N addition may promote SOC decomposition, mainly by increasing the abundance of recalcitrant C-degradation genes, whereas high N addition may inhibit SOC decomposition by decreasing the abundance of both labile and recalcitrant C degradation genes.

2. Materials and methods

2.1. Site description and soil sampling

The study was conducted at the Yi Chuan field experimental station of the Chinese Academy of Sciences on the Loess Plateau, Shaanxi Province, China (35°58′34″ N, 110°05′38.1″ E; elevation 1000–1200 m, slope 20 − 25°). The region has a classic mainland monsoon-type climate and receives an average of 584.4 mm of precipitation annually, with an average annual temperature of 9.7 °C and a frost-free period of 180 days. The soil was classified as gray forest soil (Gray Luvisols, Food and Agriculture Organization's World Soil Classification) with clay, silt, and sand contents of 36.8%, 24.3%, and 38.9%, respectively. The bulk density of the surface soil (0–20 cm) was 1.10 ± 0.03 g cm^{-3}. At the beginning of the experiment in 2014, the surface soil (0–10 cm) contained 19.87 ± 1.14 g kg^{-1} organic C, 1.46 ± 0.03 g kg^{-1} total N (TN), and 0.55 ± 0.02 g kg^{-1} total P (TP). The artificial *P. tabulaeformis* forest, with an area of 600 ha and a stand density of 1,400–1,800 trees ha^{-1}, was established in 1963. The average tree canopy density was 70%. The mean diameter at breast height and the mean tree height were 10.0 cm and 11.2 m, respectively. The stock volume was 75.5 m^3 ha^{-1}, and the leaf area index was 6.34. The understory shrubs were mainly *Elaeagnus pungens* Thunb., *Rosa xanthina* Lindl., *Spiraea salicifolia* L., *Lonicera japonica* Thunb., and *Viburnum dilatatum* Thunb., and shrub coverage was 30%. The understory herbs were mainly *Carex lanceolata* Boott and *Rubia cordifolia* L., and the herb coverage was 30–50%. The thickness of the litter layer was 5–7 cm. The climate and soil conditions of the *P. tabulaeformis* forest have good homogeneity due to the anthropogenic management after planting.

An on-going long-term N addition experiment was set up in March 2014. Based on the average ambient N deposition rate (2.2 g N m^{-2} y^{-1}) in this region (Wei et al., 2010) and the amounts of added N reported in most studies (0–12 g N m^{-2} y^{-1}) (Zhang et al., 2017a), our experiments added N as an ammonium nitrate (NH_4NO_3) solution at four N levels, each with four replicates: 0 (N0), 3 (N3), 6 (N6), and 9 (N9) g N m^{-2} y^{-1} with the same climate and terrain conditions. Four N treatments were randomly established. There was 16 plots in total, each plot was 100 m^2 (10 m × 10 m), and the plots were separated by a buffer zone of more than 5 m. Plots were sprayed with NH_4NO_3 dissolved in 10 L of distilled water before the rain at the beginning of April, June, August, and October every year. Therefore, the concentrations of ammonium nitrate solution each time are 0.0, 21.0, 41.1, 60.4 g NH_4NO_3 kg $water^{-1}$, and the corresponding total amount of N added are 0, 75, 150, 225 g N respectively. Plots receiving the N0 treatment were sprayed with an equal amount of distilled water. Spraying is an efficient way in previous field studies (Xiao et al., 2019; Yao et al., 2017). N addition experiment was applied four times a year in the growing season to evenly simulate N

deposition and reduce human error (Zhang et al., 2017a), Rain helped increase N infiltration and reduce unnecessary losses (Jing et al., 2019).

Soil samples were taken on 22 July 2018. After removing surface litter, five soil cores (5 cm inner diameter) were randomly collected from the topsoil (0–10 cm) and pooled (~1 kg). The soil samples were placed in a plastic foam box, with ice bags to ensure maintenance of an internal temperature of about 4 °C, and transported to the laboratory within one day. The samples were sieved through a 2.0-mm mesh. Part of each sample (~10 g) was frozen and stored at –80 °C for DNA extraction. The remaining part was separated into two subsamples. One subsample was air-dried and sieved through a 0.25-mm mesh for the determination of soil total organic C (SOC), TN, and TP, then sieved through a 1-mm mesh to measure nitrate-N (NO_3^--N), exchangeable ammonium-N (NH_4^+-N), available P (AP), and pH. The other subsample was stored as fresh soil at 4 °C for measuring soil water content (SWC), dissolved organic C (DOC), dissolved organic N (DON), microbial biomass C (MBC), microbial biomass N (MBN), enzyme activities, and CO_2 emissions.

2.2. Analysis of plant and soil properties

In each plot, litter samples were collected every three months from five randomly established 1 m × 1 m leaf catchers during the period July 2017 to July 2018. Root sampling was conducted in July 2018. Five 20 cm × 20 cm × 20 cm soil blocks were excavated in each plot under a randomly chosen tree and intact root segments were collected from the soil blocks. Litter and root biomass were determined after drying in an oven at 65 °C for 48 h.

Soil properties were determined using standard procedures. SWC was determined gravimetrically from 10 g soil oven-dried at 105 °C to constant weight. Soil pH was determined using a pH meter in a soil–water mix at a ratio of 1:5. SOC was measured using the H_2SO_4–$K_2Cr_2O_7$ method. TN was measured using the Kjeldahl method (Cabrera and Beare, 1993), and TP was determined colorimetrically after digestion with H_2SO_4 and $HClO_4$ (Bao, 2000). NO_3^--N and exchangeable NH_4^+-N levels were measured using a continuous-flow auto-analyzer (TRAACS 2000, Bran and Luebbe, Norderstedt, Germany). AP was extracted with 0.5 M sodium bicarbonate at pH 8.5 and measured by molybdenum–antimony colorimetry (Olsen and Sommers, 1982). Dissolved nutrients were extracted with deionized water after shaking for 1 h and then filtered through prewashed cellulose acetate filters (0.45 μm pore size). DOC contents were determined using a TOC analyzer (liqui TOC II, Elementar, Germany). Total dissolved N (TDN), NH_4^+-N, and NO_3^--N contents were determined using a continuous-flow auto-analyzer, and DON was calculated as TDN – (NH_4^+-N + NO_3^--N). Soil microbial biomass was determined by the chloroform–fumigation extraction method (Vance et al., 1987). MBC was determined using a liquid TOC analyzer at a K_{EC} (readily extractable part of microbial biomass C) of 0.38 (Joergensen, 1996). MBN was determined by ultraviolet spectrophotometry at a K_{EN} (as K_{EC}, for N) of 0.54 (Brookes et al., 1985). Soil C/N was calculated as the ratio of SOC to TN.

2.3. SOC decomposition measurement

Based on previous studies (Liu et al., 2017; Zhu et al., 2018), SOC decomposition was quantified by measuring the CO_2 emissions from soil microcosms during a 42-day incubation. Dynamic measurements were conducted to test the changes of CO_2 emission. Our lab-incubation has enough time to evaluate the patterns of SOC decomposition, and is comparable for future researches. To establish soil microcosms, 40 g (~32 g dry weight) of fresh soil were transferred into a 500-mL Mason jar (8 cm diameter, 10 cm height) and pre-incubated at 25 °C for 5 days to reduce the interference from sieving and packing, and then incubated at 25 °C in a humid environment in the dark for 42 days. Soil moisture was maintained at 60% of its water-holding capacity, based on the weighing method, by adding distilled water throughout the incubation period. To maintain aerobic conditions and reduce soil moisture loss, all jars were covered with sterile breathable sealing film except during measurements. Each treatment was replicated three times, giving a total of 48 microcosms. The incubation experiments were performed in an enclosed climate chamber (AGC-D001P, Qiushi Corp., China).

CO_2 emission rates were measured at 1, 3, 5, 7, 10, 14, 21, 28, 35, and 42 days using a Picarro G2508 $N_2O/CO_2/NH_3/CH_4/H_2O$ gas concentration analyzer (Picarro G2508 Environmental, Picarro lnc, CA, USA). During each measurement, the Mason jar was closed with a cap, which had inlet and outlet valves connected with the analyzer, so that the Mason jar and the analyzer formed a closed system. The analyzer maintained airflow throughout the system and recorded the CO_2 content every second. For each sample, we ran the measurement for 60 s, during which CO_2 efflux was not considered. The first 10 s was the preparation time for the analyzer, during which no measurements were taken. The average value of every second measurement from 11 s to 60 s was used as the CO_2 concentration in the Mason jar. Following measurement of the starting CO_2 concentration of each Mason jar, it was sealed and returned to the original incubator immediately. Two hours later, a further measurement was taken. We assumed linear CO_2 emission, and its rate was calculated as the change in CO_2 concentration during the 2-h period the jars were closed. Cumulative CO_2 emission was calculated by averaging the CO_2 emission rate between adjacent measurement dates, multiplying the average by the interval between measurements, and then summing.

2.4. Enzyme activity analyses

Hydrolytic activities of *N*-acetyl-β-glucosaminidase (EC 3.1.6.1), β-1,4-glucosidase (EC 3.2.1.21), β-xylosidase (EC 3.2.1.37), and β-D-cellulosidase (EC 3.2.1.91) were measured using a modified version of the standard fluorometric microplate assay (Marx et al., 2001). The oxidative activities of phenol oxidase (EC 1.10.3.2) and peroxidase (EC 1.11.1.7) were assayed colorimetrically using L-3,4-dihydroxyphenylalanine (L-DOPA), on a spectrophotometer of a modified version of the method of German et al. (2011). Briefly, for all enzyme assays, soil suspensions were prepared by adding 3 g of fresh soil to 125 mL of Tris-HCl buffer (pH 8.0, 50 mM) and blending thoroughly for 10 min. Assays were carried out in clear-bottom 96-well microplates. For the hydrolytic enzymes, sample reaction wells contained 150 μL of soil suspension and 50 μL of enzyme substrate; homogenate control wells contained 150 μL of soil suspension and 50 μL of buffer; negative control wells contained 150 μL of buffer and 50 μL of enzyme substrate; quench control wells contained 150 μL of soil suspension and 50 μL of MUB standard; standard wells contained 150 μL of buffer and 50 μL of MUB standard. The plates were incubated at 25 °C for 4 h (2 h for β-1,4-glucosidase) and then spectrophotometrically analyzed at 365 nm excitation and 450 nm emission. For the oxidative enzymes, phenol oxidase assay wells contained 200 μL of soil suspension and 50 μL of L-DOPA; peroxidase assay wells contained 200 μL of soil suspension, 50 μL of L-DOPA, and 0.3% H_2O_2; blanks contained 150 μL of soil suspension and 50 μL of buffer. The plates were incubated at 25 °C for 4 h, centrifuged at 3,600 rpm for 5 min, and the absorbance at 460 nm was read. The activity of hydrolytic and oxidative enzymes (nmol g^{-1} dry soil h^{-1}) were calculated as described by German et al. (2011) and Bach et al. (2013).

2.5. Microbial C-cycling functional gene analyses

Microbial DNA was extracted from 0.5 g of soil using the MoBio PowerSoil DNA isolation kit (MoBio Laboratories, Carlsbad, CA, USA) according to the manufacturer's protocol. DNA quality was assessed based on the 260/280 nm and 260/230 nm absorbance ratios. DNA was quantified with the PicoGreen method (Ahn et al., 1996) and stored at −20 °C until use. The soil microbial functional gene diversity and composition were profiled using GeoChip 5.0 according to Zhang et al. (2017a). We mainly focused on functional genes associated with C-cycling. Briefly, purified DNA (500 ng) was labeled with the fluorescent

dye Cy-3 by random priming. The labeled DNA was mixed with 42 μL of buffer and incubated at 95 °C for 3 min, then hybridized to the microarray, which was scanned using a NimbleGen MS200 Microarray Scanner (Roche NimbleGen, Inc., Madison, WI, USA) at 633 nm. The images were converted, digitized, processed, and analyzed using ImaGene 6.0 software. For quality control, based on the raw data, the signal-to-noise ratio (SNR) was adjusted and poor-quality spots with an SNR < 2.0 were removed. The signal intensity of each probe was then log-transformed and divided by the average signal intensity in the sample to standardize the data, and probes that appeared in only one of four replicates of each treatment were removed as noise, to obtain normalized data. The normalized data were used to profile C-cycling functional gene composition and to calculate alpha diversity. Gene intensities normalized to total signal intensity were used to analyze the relative abundance of each gene category or family in each sample.

2.6. Statistical analysis

All data were reported as the mean ± standard deviation for four replicates. One-way analysis of variance (ANOVA) and least-significant difference tests at the 5% level of significance were performed to examine significant differences in soil properties, plant biomass, C-cycling functional gene abundance, enzyme activities, and CO_2 emission among the various N treatments. All statistical analyses were conducted using SPSS 19.0 (SPSS, Inc., Chicago, IL, USA). Principal coordinate analysis (PCoA) was performed to reveal overall changes in C-cycling functional gene composition induced by N addition. Permutational multivariate analysis of variance (Adonis), analysis of similarities (ANOSIM), and a multi-response permutation procedure (MRPP) function were used to test the significance of the changes based on a Bray–Curtis dissimilarity matrix of C-cycling functional genes. Redundancy analysis (RDA) was applied to investigate correlations between C-cycling functional gene changes and environmental factors (soil properties and plant biomass). The Mantel test was used to examine correlations among Bray–Curtis distances for C-degradation genes, Euclidean distances for soil properties, plant biomass, enzyme activities, and cumulative CO_2 emission based on the Spearman correlation coefficient. All the above statistical analyses were conducted using the Vegan package in R (v 3.6.0). Linear regression analysis was used to fit cumulative CO_2 emissions or enzyme activities to C-degradation gene abundance. $P < 0.05$ was considered significant. Pearson correlation analysis was performed to explore relationships between variables. Partial least squares path modeling (PLS-PM) was performed to further evaluate the direct and indirect effects of soil properties, plant biomass, enzyme activities, and C-degradation genes on CO_2 emissions (R plspm package). Path coefficients and explained variability (R^2) reflected cause-and-effect relationships among observed and latent variables. A goodness-of-fit (GOF) test was used to evaluate the overall predictive power of the model.

3. Results

3.1. Effects of N addition on soil properties, microbial biomass, and plant biomass

After 5 years of N addition, soil properties and microbial biomass showed significant differences across all N addition treatments (Table 1). NO_3^--N and DON contents were consistently elevated with increasing N addition levels. SOC and DOC contents and the soil C/N ratio initially increased and then decreased with increasing N addition levels, and the highest values of SOC and soil C/N were observed in the N6 treatment, whereas the highest DOC value was observed in the N3 treatment. Other soil properties, including TN, TP, exchangeable NH_4^+-N, AP, and pH, showed no significant difference among all treatments ($P > 0.05$). MBC and MBN initially increased and then decreased in all N addition treatments, with the maximum observed in the N6 treatment, but only changes in MBC were significant ($P < 0.05$). N addition had no significant effects on litter and root biomass ($P > 0.05$).

Table 1
Soil properties, microbial biomass, and plant biomass in different N addition treatments.

Environmental attributes	N0	N3	N6	N9
SOC (g kg^{-1})	19.92 ± 0.60b	21.34 ± 1.62ab	22.78 ± 0.77a	20.78 ± 1.64ab
TN (g kg^{-1})	1.46 ± 0.03a	1.47 ± 0.02a	1.52 ± 0.02a	1.56 ± 0.14a
TP (g kg^{-1})	0.54 ± 0.01a	0.55 ± 0.02a	0.52 ± 0.01a	0.56 ± 0.03a
NO_3^--N (mg kg^{-1})	19.27 ± 1.61c	23.79 ± 2.2bc	26.27 ± 3.0ab	29.88 ± 5.0a
exchangeable NH_4^+-N (mg kg^{-1})	2.03 ± 0.63a	1.77 ± 0.03a	1.74 ± 0.23a	1.59 ± 0.08a
AP (mg kg^{-1})	3.56 ± 0.65a	3.19 ± 1.15a	2.63 ± 0.65a	3.94 ± 1.02a
pH	7.62 ± 0.18a	7.75 ± 0.05a	7.76 ± 0.04a	7.71 ± 0.14a
DOC (mg kg^{-1})	183.99 ± 14.25a	196.99 ± 20.43a	146.03 ± 22.60b	138.59 ± 21.46b
DON (mg kg^{-1})	3.24 ± 0.58b	3.29 ± 0.63b	4.09 ± 0.50ab	4.5372 ± 0.44a
Soil C/N	13.62 ± 0.55b	14.52 ± 1.24ab	14.95 ± 0.44a	13.35 ± 0.56b
MBC (mg kg^{-1})	567.41 ± 59.72b	630.92 ± 78.68b	734.42 ± 60.84a	644.92 ± 36.31ab
MBN (mg kg^{-1})	79.99 ± 4.60a	81.39 ± 10.04a	86.33 ± 7.77a	85.39 ± 9.30a
Litter biomass (g m^{-2} y^{-1})	210.41 ± 14.39a	189.60 ± 8.15a	186.69 ± 22.22a	182.05 ± 20.66a
Root biomass (g m^{-2})	76.91 ± 6.63a	75.06 ± 7.20a	74.53 ± 7.41a	74.52 ± 6.80a

SOC, total soil organic C; TN, total N; TP, total P; NO_3^--N, nitrate nitrogen; NH_4^+-N, ammonium nitrogen; AP, available P; DOC, dissolved organic C; DON, dissolved organic N; Soil C/N, the ratio of SOC and TN; MBC, microbial biomass C; MBN, microbial biomass N; All data are presented as mean ± SD (n = 4). Different letters indicate significant ($P < 0.05$) differences among treatments. The treatments N0, N3, N6, and N9 represent the applied N rates of 0, 3, 6 and 9 g m^{-2} y^{-1}, respectively.

3.2. Effects of N addition on overall soil microbial functional diversity and community in the C-cycle

In total, 17,830 hybridized functional gene probes, representing 122 genes associated with C fixation, C degradation, and methane emission, were detected (Table S1). The abundance and diversity (Shannon–Wiener index) of functional genes increased with added N up to the N6 treatment, and significantly decreased under the N9 treatment ($P < 0.05$, Table 2), with the highest and lowest values observed in N6 and N9, respectively. Evenness (Pielou index) exhibited an opposite trend (Table 2). The MRPP, Adonis, and ANOSIM results showed that the overall functional gene composition varied significantly with N addition treatments ($P < 0.05$, Table S2). A PCoA ordination plot (Fig. 1A) shows the differences between C-cycling functional gene communities following different N addition treatments, with the first two principal coordinates explaining 66.24% and 10.94% of the total functional gene composition variation. The horizontal axis clearly separates C-cycling functional genes by N addition, and the N0, N3, and N6 treatments are distributed along the left side of the Y axis, whereas the N9 treatment is on the right side. The Bray–Curtis dissimilarity values for functional gene composition increased with increasing N addition levels. Compared to N3 and N6, N9 was less similar to N0 (Fig. 1B). Thus, the treatments were divided into low-N (N3 and N6) and high-N (N9) treatments. RDA revealed that environmental attributes explained 51.67% of the variation in the C-cycling functional gene composition of microbial communities (Fig. 2). Among all factors evaluated, functional

Table 2
Soil microbial C-cycling functional genes abundance, diversity and evenness in different N addition treatments.

Treatment	Genes abundance(signal intensities of probes detected)				Shannon-Wiener index (H')	Pielou evenness index(E_H)
	C-cycling	C-fixation	C-degradation	Methane		
N0	**15,932 ± 486a**	4,046 ± 121a	11,570 ± 354b	315.43 ± 11.43a	**8.87 ± 0.03b**	**0.99820 ± 0.00006b**
N3	**16,470 ± 347a**	4,159 ± 88a	11,986 ± 254ab	324.23 ± 5.14a	**8.91 ± 0.02ab**	**0.99818 ± 0.00005b**
N6	**16,639 ± 95a**	4,205 ± 49a	12,108 ± 143a	325.64 ± 3.61a	**8.92 ± 0.01a**	**0.99817 ± 0.00006b**
N9	**13,908 ± 679b**	3,563 ± 175b	10,088 ± 490c	257.48 ± 5.95b	**8.74 ± 0.04c**	**0.99845 ± 0.00011a**

All data are presented as mean ± SD (n = 4). Different letters indicate significant ($P < 0.05$) differences among treatments.

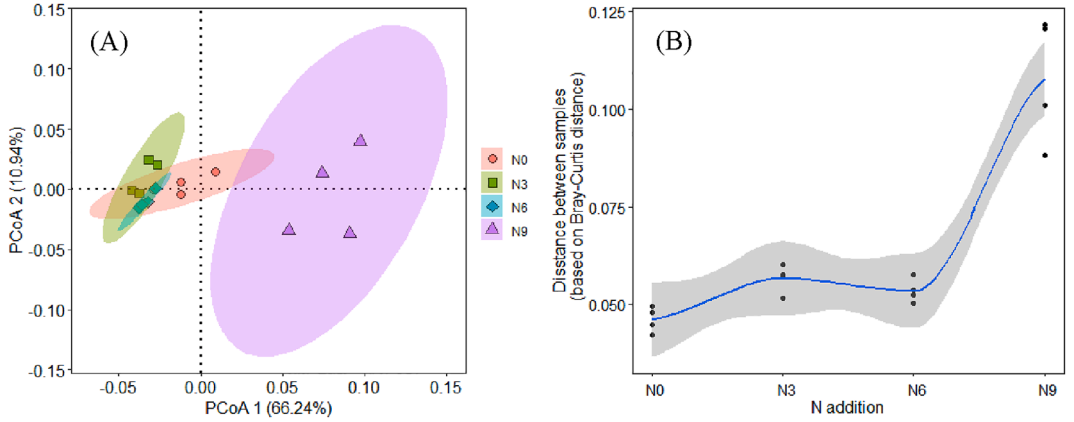

Fig. 1. Principal coordinate analysis (PCoA) of all detected C-cycling functional genes compositions based on normalized signal intensity from different N addition treatments (A). Regression analysis of N addition and functional genes distance (based on Bray-Curtis distances) (B).

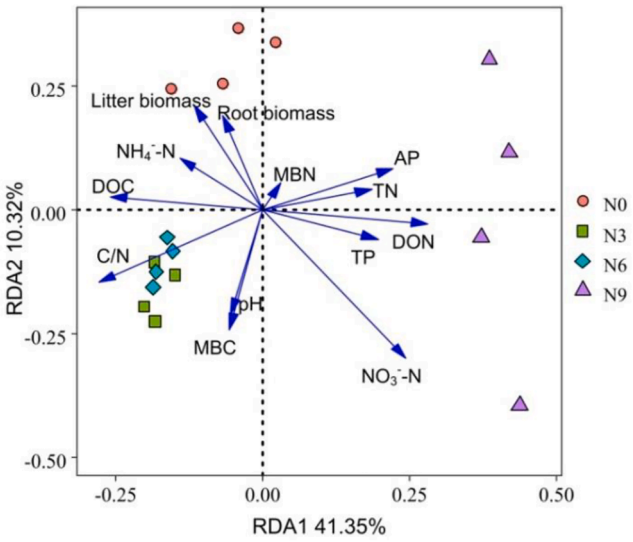

Fig. 2. Redundancy analysis (RDA) of C-cycling functional genes community based on normalized signal intensity from different N addition treatments. The arrows indicate the lengths and angles between explanatory and response variables and reflect their correlations.

gene composition changes were significantly correlated with NO_3^--N, MBC, DOC, and DON content.

3.3. Effects of N addition on key functional genes involved in the C-cycle

In all treatments, C-cycling functional gene communities were predominantly composed of C-degradation genes, accounting for 72.43–72.82%. At the gene subcategory level (Fig. 3), the abundances of functional genes involved in the degradation of various C compounds (from labile to recalcitrant C, including starch, hemicellulose, pectin, cellulose, chitin, vanillin/lignin, and lignin) increased under low N addition (N3 and N6) and decreased under high N addition (N9). However, significant differences were observed only in the abundances of genes involved in pectin degradation under N3, and in starch, pectin, and chitin degradation under N6 ($P < 0.05$), whereas there was no significant effect on those of genes involved in the recalcitrant C (vanillin/lignin, lignin) degradation ($P > 0.05$). High N addition had significant negative effects on the abundances of genes involved in the degradation of all C compounds ($P < 0.05$; Fig. 3). At the individual gene level (Fig. 4), C-degradation gene abundance under N3 treatment increased by 4.35% on average, and 4 out of the 27 genes (only those genes that accounted for > 10% of the various C compound degradation gene abundance are shown), including *pula* for starch degradation and *pec-CDeg*, *pme*, and *rgl* for pectin degradation, were present at significantly higher levels ($P < 0.05$, Fig. 4A). Likewise, the abundance of C-degradation genes increased by 4.93%, on average, under N6 treatment, and 16 out of the 27 genes, including most genes involved in labile C decomposition (e.g., *amyA*, *glucoamylase*, *pula*), and few recalcitrant C decomposition genes (*vana*, *phenol-oxidase*), were present at significantly higher levels ($P < 0.05$; Fig. 4B), whereas the abundance of all C-degradation genes decreased by 12.73%, on average, under N9 treatment ($P < 0.05$; Fig. 4C).

3.4. Effects of N addition on SOC-degrading enzyme activities

N addition had significant effects on oxidase and hydrolase activities ($P < 0.05$; Fig. 5). Phenol oxidase activity increased under low N addition and significantly decreased under high N addition ($P < 0.05$; Fig. 5A), whereas N addition had no significant effect on peroxidase activity ($P > 0.05$; Fig. 5B). All hydrolases except *N*-acetyl-β-glucosaminidase showed a similar trend (Fig. 5C-F). N6 treatment significantly enhanced β-D-cellulosidase activity by 38.35%, and N9 significantly suppressed β-xylosidase activity by 43.49%. β-1,4-glucosidase activity was not significantly affected by N addition. Interestingly, *N*-acetyl-β-glucosaminidase activity decreased with increasing N addition and

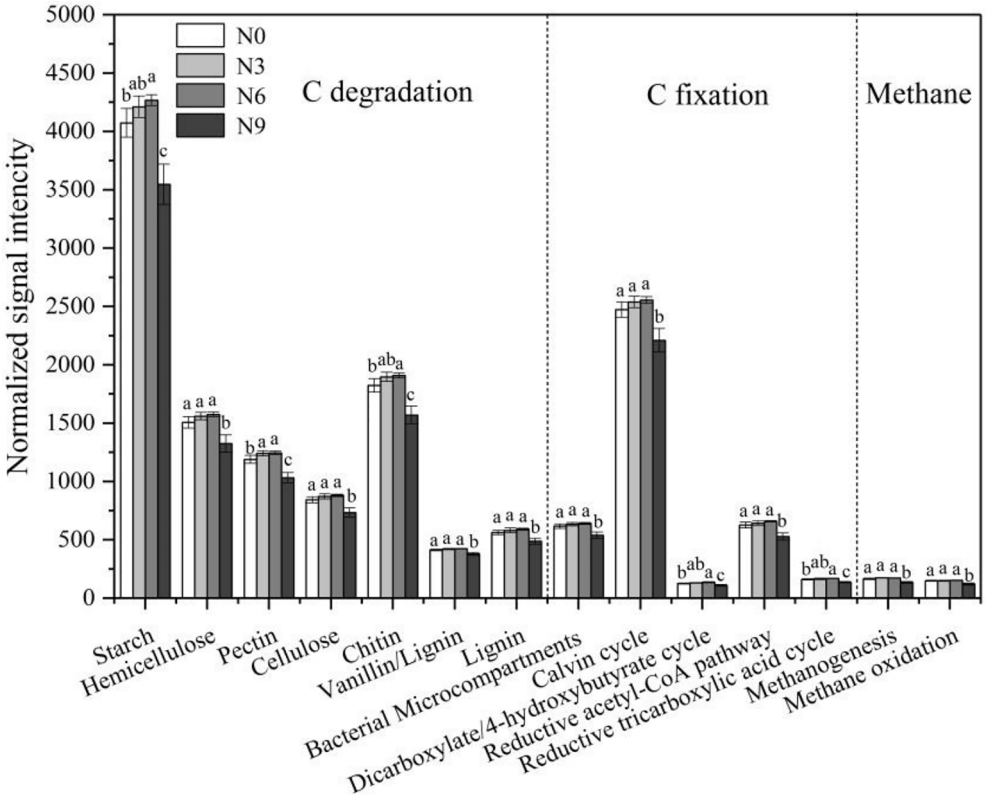

Fig. 3. The abundance of detected functional genes involved in C-cycling at the gene subcategory level in different N addition treatments. Different letters indicate significant ($P < 0.05$) differences among treatments. Error bars represent standard error (n = 4).

was significantly suppressed by 49.77% under N9.

3.5. Effect of N addition on CO_2 emission

During the 42-day incubation, the temporal pattern of the CO_2 emission rates was similar among the different N addition treatments, with the highest CO_2 emission rate on the third day and a gradual decrease thereafter. Specifically, the emission rate was relatively high during the first 10 days, and then stabilized at a lower level (Fig. 6A). Cumulative CO_2 emissions initially increased and then decreased with increasing N addition levels. The lowest and highest cumulative CO_2 emissions were observed under N9 and N6, respectively. The cumulative CO_2 emissions ranged from 6.18% of the SOC to 7.28% of the SOC (Fig. 6B).

3.6. Relationships of CO_2 emissions with the abundances of C-degradation genes and SOC-degrading enzyme activities

Mantel test results indicated a strong correlation between SOC-degrading enzyme activities and the C-degradation gene community composition, and both of them were significantly related to soil properties, but not plant properties (Table 3). Importantly, cumulative CO_2 emission was significantly correlated with both SOC-degrading enzyme activities and the composition of the C-degradation gene community. Pearson analysis produced similar results in that significant correlations were found between cumulative CO_2 emissions and C-degradation gene abundance and SOC-degrading enzyme activities (Table S3). We also observed a strong positive linear correlation between cumulative CO_2 emission and C-degradation gene abundance (Fig. S1a), a negative linear relationship between the first principal coordinate of C-degradation gene communities and the first principal coordinate of SOC-decomposing enzyme activities (Fig. S1b), and a strong positive linear correlation between the relative abundance of acetylglucosaminidase encoding genes and the activity of acetylglucosaminidase, xylanase encoding genes and xylanase activity, and exoglucanase encoding genes and exoglucanase activity (Fig. S1c-e; all $P < 0.05$). PLS-PM analysis revealed that N addition significantly, if indirectly, affected C-degradation gene community composition and SOC-degrading enzyme activities by its direct effects on environmental variables (Fig. 7). The direct effects of C-degradation gene community composition on CO_2 emissions and indirectly by affecting SOC-degrading enzyme activities were apparently significant. Among all variables, C-degradation gene community composition had the strongest influence on CO_2 emission.

4. Discussion

4.1. Effect of N addition on microbial C-cycling functional genes

In our field study, N addition significantly altered the composition of the microbial C-cycling functional gene assemblage (Fig. 1A, Table S2); low N addition resulted in higher abundance and diversity of functional genes, whereas under high N addition these had significantly lower values (Table 2), which supported our first hypothesis.

Relatively low levels of N addition are considered to enhance microbial functional gene abundance (Freedman et al., 2013). Consistent with the finding, we observed an increase in C-cycling functional gene abundance and diversity under low N addition. Generally, in N-limited ecosystems, plant growth and microbial activity are limited by N supply; low N addition would increase soil microbial biomass and functional potential directly by increasing N availability or indirectly by increasing nutrient availability through promoting plant productivity and C inputs from aboveground plant components (Magnani et al., 2007; Wang et al., 2019b). Our results generally supported this view, as we found that low N addition resulted in significantly higher soil NO_3^--N, SOC, DOC, MBC, and C/N ratio (Table 1; Fig. 2). However, although plant litter and root exudates are the two major C sources for microbial activities (Garcia-

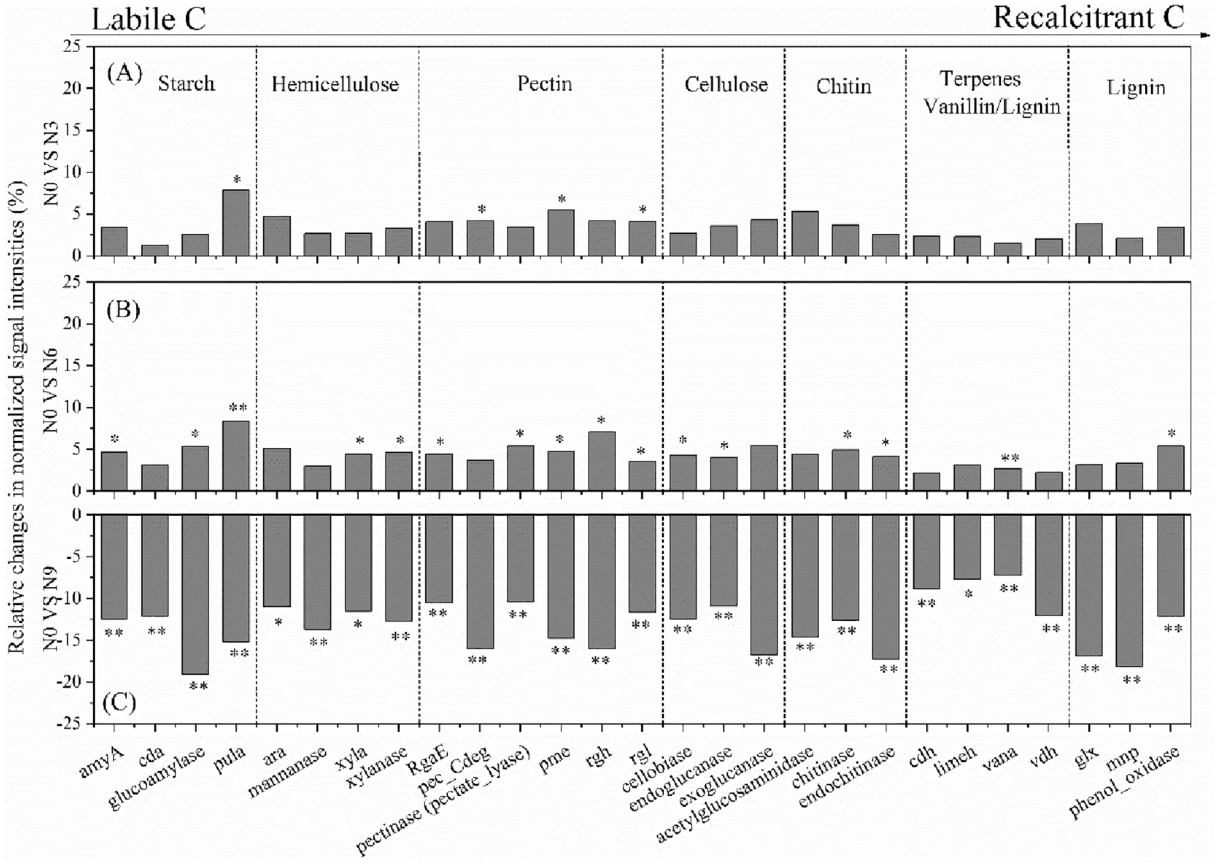

Fig. 4. The relative changes of the abundance of detected functional genes involved in C substrate degradation in the N3 (A), N6 (B) and N9 (C) compared with N0 treatment respectively. The complexity of C substrate is presented in order from labile to recalcitrant from left to right. The differences between N addition and N0 treatment were tested by independent-samples T tests, and symbols ** and * indicated significant differences at $P < 0.01$ and $P < 0.05$ respectively.

Palacios et al., 2016), in our study, litter and root biomass did not increase under low N addition (Table 1) and were not associated with changes in functional gene abundance and composition (Fig. 2; Table 3). This indicated a slow response of the mature artificial *P. tabulaeformis* forest to N addition and that N addition in the short 5-year experimental period did not change above- and belowground productivity. In addition, with a stand age of 60 years, the litter layer covering the soil in the forest is relatively thick, with a slow turnover rate, and thus, the effect of the new litter layer on C input is limited. Another study in this region showed that short-term low N addition enhanced fine root decomposition and compound release (Jing et al., 2019), which may be the main reason for the increase in C input. In some studies, increases in soil C content were also significantly correlated with fine root production and turnover, but not with aboveground input (Norby et al., 2004). It should be noted that low N caused significantly greater abundance of specific genes, but the effect of low N on the total abundance and diversity of C-cycling functional gene was not significant. This finding is consistent with the work of Li et al. (2019), who found that soil bacterial communities did not significantly differ among the fertilization treatments after 3-year N addition. The low dose and short period (3 or 5 years) of N addition may be a major explanatory factor in these unexpected non-significant responses of the soil microbial community.

In addition, the increased N addition could induce a change in the N state in the ecosystem from limitation to saturation, and the soil microbial biomass and functional potential responses may gradually change from increasing to decreasing (Chen et al., 2015; Li et al., 2020). For example, Liu et al. (2014) observed that microbial biomass began decreasing when the amount of added N was increased to 8 g N m^{-2} y^{-1} in a temperate steppe in northern China. Zhang et al. (2017a) reported that the addition of 2.5 g N m^{-2} y^{-1} was the ecosystemic threshold in a perennial herb ecosystem on the Loess Plateau, above which N addition exerted an inhibitory effect on microbial biomass and activity. Other N addition experiments in this region showed that soil aggregate stability, SOC content, and easily extractable glomalin-related soil protein increased from the 0 to 6 g N m^{-2} y^{-1} treatments, and were decreased under the 9 g N m^{-2} y^{-1} treatment (Sun et al., 2018; Yao et al., 2017). Thus, we speculate that 9 g N m^{-2} y^{-1} exceeds the critical N requirement for plants and microbes on the Loess Plateau and therefore has an adverse effect on microbial activity. We also observed a significant decrease in C-cycling functional gene abundance and diversity under N9 (Table 2). Importantly, the critical value at which a change in ecosystemic N status occurs is influenced by climate conditions, vegetation types, ecosystem type, and other factors. Further, N saturation contents that plants, soil, and microbes can endure vary, even within the same ecosystem and region.

The decreases in C-cycling functional gene abundance and diversity under high N addition in our study may be related to the significant decreases in DOC and MBC (Fig. 2; Table 1), which may be caused by a reduction in underground resource allocation in plants under high N addition treatment (Treseder, 2004). Previous studies have revealed that underground C allocation is inversely proportional to N availability (Bae et al., 2015). Generally, low pH is thought to inhibit microbial activity and diversity under high N addition or in N-saturated ecosystems (Mao et al., 2017). However, this was not the case in our study as N addition hardly affected the pH, which ranged from 7.37 to 7.85, and RDA showed that pH had no significant effect on functional gene communities. Probably, the N addition period was too short to have an observable cumulative effect on pH. Accordingly, we speculate that the soil may acidify and eventually inhibit microorganisms under long-term N addition. Overall, our results indicated that changes in soil resource

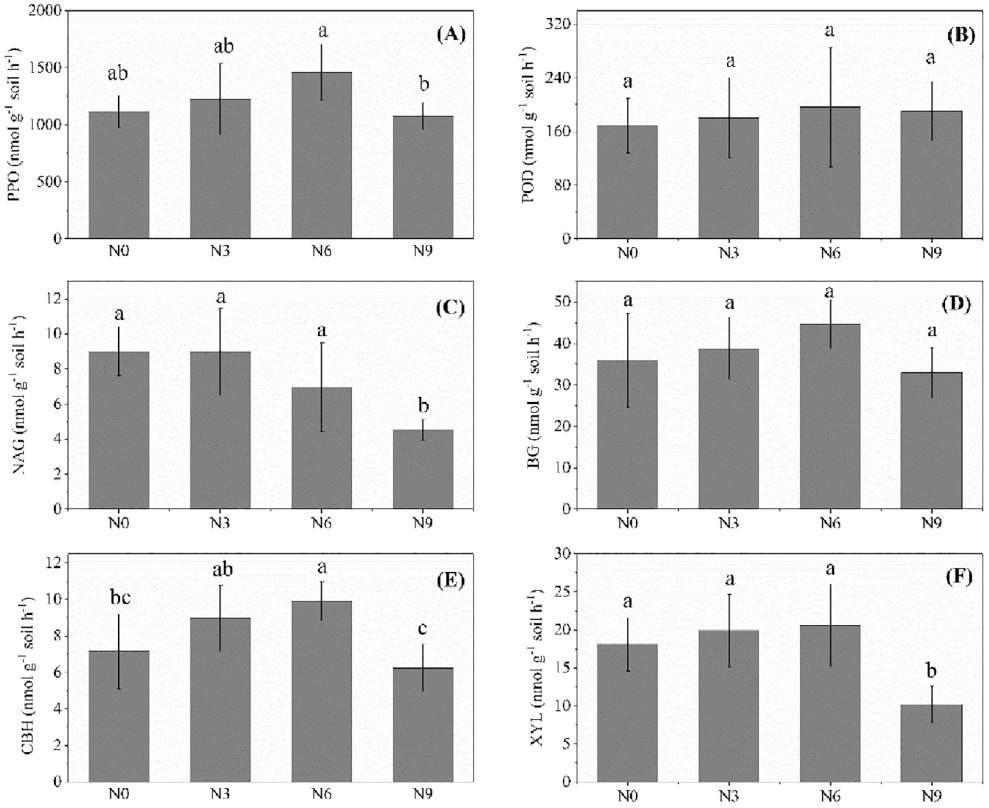

Fig. 5. Activities of polyphenol oxidase (PPO) (A), peroxidase (POD) (B), *N*-acetyl-β-glucosaminidase (NAG) (C), β-1,4-glucosidase (BG) (D), β-D-cellulosidase (CBH) (E), β-xylosidase (XYL) (F) in different N addition treatments. Different letters indicate significant ($P < 0.05$) differences among treatments. Error bars represent standard error (n = 4).

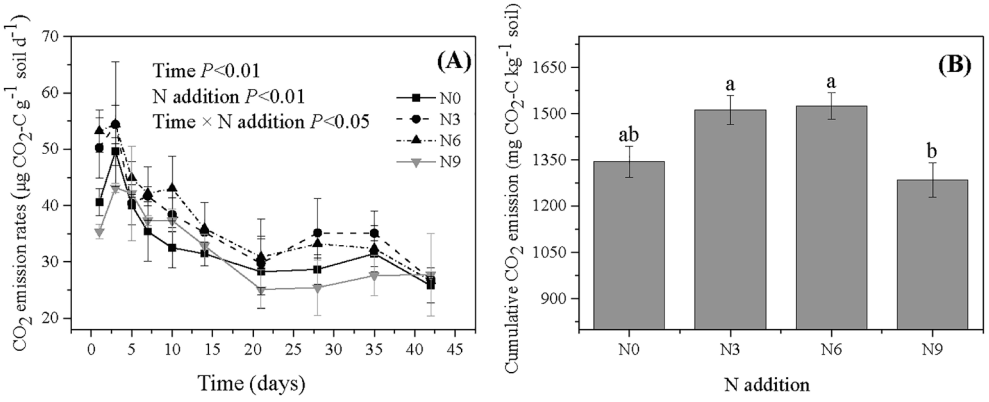

Fig. 6. The temporal patterns of CO_2 emission rates (A) and cumulative CO_2 emission during the 42-day incubation (B) in different N addition treatments. Different letters indicate significant ($P < 0.05$) differences among treatments. Error bars represent standard error (n = 4).

Table 3
Mantel test results that were used to discern correlations among the C-degradation genes Bray-Curtis distances, soil properties (SOC, NO_3^--N, DOC, DON, MBC and soil C/N; other non-significant soil properties were not analyzed), enzyme activities (PPO, NAG, CBH and XYL), plant variables (Litter biomass, Root biomass) and cumulative CO_2 emission Euclidean distances. The values shown are correlation coefficients based on the Spearman method. * indicates $P < 0.05$; ** indicates $P < 0.01$.

	Soil properties	Plant variables	Cumulative CO_2 emission	Enzyme activities	C-degradation genes
Soil properties	1				
Plant variables	0.046	1			
Cumulative CO_2 emission	−0.048	−0.037	1		
Enzyme activities	**0.213***	−0.007	**0.271****	1	
C-degradation genes	**0.242***	0.048	**0.360****	**0.504****	1

SOC, total soil organic carbon; NO_3^--N, nitrate nitrogen; DOC, dissolved organic carbon; DON, dissolved organic nitrogen; MBC, microbial biomass C; Soil C/N, the ratio of SOC and TN; PPO, polyphenol oxidase; NAG, *N*-acetyl-β-glucosaminidase; CBH, β-D-cellulosidase; XYL, β-xylosidase.

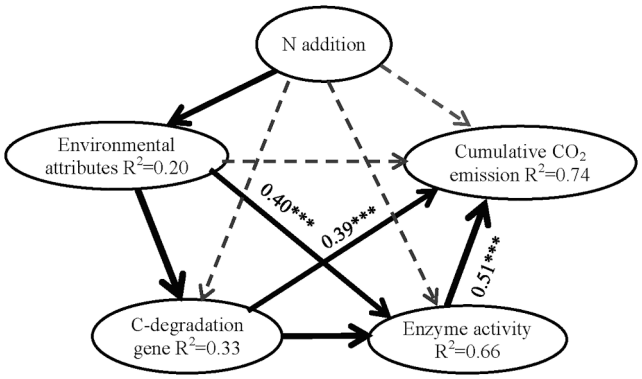

Fig. 7. Path analysis diagrams based on the partial least squares path model (PLS-PM) for CO_2 emission. Each box represents an observed variable (i.e., measured) or latent variable (i.e., constructs). Path coefficients are calculated after 1000 bootstraps and reflected in the width of the arrows; dashed arrows indicate that the path coefficients between latent variables are not significant. Environmental attributes: SOC, NO_3^--N, DOC, DON, MBC and soil C/N; other non-significant factors were not analyzed. C-degradation gene: the first two principal coordinate axes scores (PCoA1 and PCoA2) of principal coordinate analysis (PCoA) scores of functional gene communities, enzyme activity: phenol oxidase, *N*-acetyl-β-glucosaminidase, β-D-cellulosidase and β-xylosidase.

availability caused by cumulative effects of low or high N addition more strongly affect microbial functional gene composition and diversity than does soil acidification, and the effect depends on the amount of added N. Based on the current N deposition level in the Loess hill-gully region, we speculate that microbial C-cycling functional gene diversity and metabolic potential will increase and may accelerate soil C-cycling in the forest ecosystem.

Interestingly, we found that the abundances of labile and recalcitrant C-degradation genes were differentially affected in terms of abundance by N addition. N3 and N6 addition resulted in significantly higher abundances of 4 and 16 out of 27 C-degradation genes mainly involved in the degradation of relatively labile C (starch, pectin, and chitin), respectively. Although low N addition also caused significantly greater abundance of a few recalcitrant C degradation genes, such as *vana* for vanillin, and *phenol-oxidase* for lignin, these differences did not reach significance at the gene subcategory level (Fig. 3A-B). This suggests that the abundances of labile C degradation genes are more sensitive to low N addition than those of recalcitrant C degradation genes, thus contradicting our second hypothesis, and may be partially attributable to the increase in labile C under low N addition (Huang et al., 2019). In addition, microbial taxonomic gene sequencing studies have shown that N addition promoted copiotrophic rather than oligotrophic taxa (Zeng et al., 2016) with a shift towards labile C decomposition (Fierer et al., 2012), which is in line with our results. Consistent with our initial hypothesis, high N addition caused significantly lower abundance of all the C-degradation genes evaluated (Fig. 3C), which is also consistent with findings reported by Eisenlord et al. (2013). This may be because of the overall decrease in C-cycling functional gene abundance under high N addition.

4.2. Effect of changes in soil microbial C-degradation functional potentials on SOC decomposition

Our results showed that low N addition promoted SOC decomposition mainly by increasing the abundance of labile rather than recalcitrant C degradation genes, while high N addition decreased SOC decomposition by decreasing the abundance of both labile and recalcitrant C-degradation genes. These results are partially consistent with our second hypothesis.

In the present study, SOC decomposition was not measured directly, but was indirectly assessed by monitoring CO_2 emissions. We considered this to be reasonable because soil CO_2 emissions are partly autotrophic in nature (e.g., root, mycorrhizal, and rhizosphere respiration), but mainly heterotrophic, as microbes consume organic C and release CO_2 into the atmosphere (Zhou et al., 2014). The incubation experiment was conducted in the absence of plants, to exclude any influence of roots, mycorrhizae, and root exudates on soil C decomposition. Therefore, the amount of C released from the soil represented the amount of SOC decomposed by microorganisms (Xu et al., 2019). Our results showed that low N addition resulted in higher CO_2 emissions, whereas high N addition caused lower CO_2 emissions (Fig. 6B). The responses of SOC-degrading enzyme activities, including phenol oxidase, peroxidase, β-1,4-glucosidase, β-D-cellulosidase, and β-xylosidase, to N addition were in line with CO_2 emissions (Fig. 5). Together, these results indicated that low N addition may promote SOC decomposition, whereas high N addition may inhibit SOC decomposition, which is in agreement with our second hypothesis. This is also supported by previous studies; in N-limited ecosystems, such as the Loess Plateau, the semiarid grasslands in Inner Mongolia, and the alpine steppe in northern Tibet, soil respiration is stimulated by relatively low-level N addition (no >10 g m^{-2} y^{-1}), and inhibited by high-level N addition (Zhu et al., 2016). The differences in the ecosystemic N status caused by low and high N addition are probably largely responsible for these differences in SOC decomposition.

Microorganisms are key drivers of the Earth's biogeochemical cycles (Bani et al., 2018; Falkowski et al., 2008); they regulate litter decomposition, soil nutrient cycling, and other important biochemical functions. In our study, the abundance of C-degradation genes encoding enzymes for the decomposition of starch, (hemi-) cellulose, chitin, lignin, and other C compounds was higher under low N addition and significantly lower under high N addition, indicating differential functional potentials of microorganisms for C decomposition under these conditions. Interestingly, we found that the changes in CO_2 emissions and SOC-degrading enzyme activities occurred in parallel and were significantly correlated with the changes in C-degradation gene abundance and composition (Table 3, Fig. S1). These results provide an indirect evidence that changes in microbial C-degradation genes composition and metabolic potential paralleled functional responses of the soil. PLS-PM further indicated that N addition specifically induced changes in microbial C-degradation gene community composition, which directly or indirectly regulated SOC decomposition by affecting SOC-decomposing enzyme activities (Fig. 7). This finding was consistent with a previous study reporting that a decrease in microbial C-cycling gene abundance induced a slowdown of litter decomposition and an increase in soil C storage during vegetation succession (Zhong et al., 2018). Combined with the effect of N addition on labile and recalcitrant C degradation gene abundances, all these changes indicated that low N addition increased SOC decomposition primarily via higher microbial functional potentials for degrading labile C, whereas high N addition decreased SOC decomposition primarily via lower microbial functional potentials for degrading both labile and recalcitrant C, which partly supports our second hypothesis.

Some studies have suggested that coarse measures of microbial functional traits based on DNA are not always correlated with changes in ecological functional processes (Rocca et al., 2015; Wood et al., 2015). One reason for this gene-process decoupling may be that the presence of potential functional genes does not always represent actual functionality of microorganisms (Nannipieri et al., 2019). Before the final enzyme-catalyzed chemical reactions can occur, gene transcription and protein synthesis are required, and functional processes are likely controlled by the expression rather than the overall abundance of related genes (Levy-Booth et al., 2014). The other reason may be that any ecosystem process is a result of the combined effects of biological and non-biological factors, such as climate, vegetation, soil, microorganisms, and other ecosystemic processes. It is difficult to represent an accurate measure to correlate such complex ecosystem processes with functional gene abundance. Therefore, we tested the microbial functional genens,

enzyme activities, and CO_2 emissions in the present study to persuasively evaluating the mechanism of SOC decomposition. Further observation of each study system is required to elucidate gene abundance roles in the microbial biogeochemical process.

5. Conclusions

Forests are one of the ecosystems severely affected by N deposition. The present study confirmed that there is a threshold effect of N addition on SOC decomposition. From the perspective of microbial functional potential, we try to find the mechanisms for these results. Low N addition had a positive effect on labile C-degradation gene abundance, but no significant effect on recalcitrant C-degradation gene abundance. High N addition significantly decreased the abundance of functional gens. Labile C-degradation gene is the main driving factor for SOC decomposition changes, while soil recalcitrant C pool may not be activated by the microbial community and N addition, and the stability of soil C sequestration may not be altered under long-term N deposition. Using GeoChip 5.0, our study provide solid evidences for the different results of SOC decomposition in previous studies.

CRediT authorship contribution statement

Hang Jing: Writing – review & editing. **Jingjing Li:** Data curation, Writing - original draft. **Benshuai Yan:** Software, Investigation. **Furong Wei:** Visualization, Data curation. **Guoliang Wang:** Conceptualization, Methodology. **Guobin Liu:** Supervision, Project administration.

Declaration of Competing Interest

The authors declare that they have no known competing financial interests or personal relationships that could have appeared to influence the work reported in this paper.

Acknowledgements

Supported by the National Natural Science Foundation of China (No. 41671513); National Key Research and Development Program of China (2017YFC0504601).

Data availability

GeoChip data are available online (www.ncbi.nlm.nih.gov/geo/) with the accession number GSE147041.

Appendix A. Supplementary material

Supplementary data to this article can be found online at https://doi.org/10.1016/j.foreco.2021.119098.

References

Ahn, S.J., Costa, J., Emanuel, J.R., 1996. PicoGreen quantitation of DNA: effective evaluation of samples pre- or post-PCR. Nucleic Acids Res. 24, 2623–2625. https://doi.org/10.1093/nar/24.13.2623.

Bach, C.E., Warnock, D.D., Van Horn, D.J., Weintraub, M.N., Sinsabaugh, R.L., Allison, S. D., German, D.P., 2013. Measuring phenol oxidase and peroxidase activities with pyrogallol, L-DOPA, and ABTS: Effect of assay conditions and soil type. Soil Biol. Biochem. 67, 183–191. https://doi.org/10.1016/j.soilbio.2013.08.022.

Bae, K., Fahey, T.J., Yanai, R.D., Fisk, M., 2015. Soil nitrogen availability affects belowground carbon allocation and soil respiration in Northern hardwood forests of New Hampshire. Ecosystems 18, 1179–1191. https://doi.org/10.1007/s10021-015-9892-7.

Bani, A., Pioli, S., Ventura, M., Panzacchi, P., Borruso, L., Tognetti, R., Tonon, G., Brusetti, L., 2018. The role of microbial community in the decomposition of leaf litter and deadwood. Appl. Soil Ecol. 126, 75–84. https://doi.org/10.1016/j.apsoil.2018.02.017.

Bao, S.D., 2000. The determination of phosphorus in the soil. In: 3 (Ed.), Soil and Agricultural Chemistry Analysis. China Agriculture Press, Beijing, pp. 74-76.

Bardgett, R.D., Freeman, C., Ostle, N.J., 2008. Microbial contributions to climate change through carbon cycle feedbacks. ISME J. 2, 805–814. https://doi.org/10.1038/ismej.2008.58.

Brookes, P.C., Landman, A., Pruden, G., Jenkinson, D.S., 1985. Chloroform fumigation and the release of soil nitrogen: a rapid direct extraction method to measure microbial biomass nitrogen in soil. Soil Biol. Biochem. 17, 837–842. https://doi.org/10.1016/0038-0717(85)90144-0.

Cabrera, M.L., Beare, M.H., 1993. Alkaline persulfate oxidation for determining total nitrogen in microbial biomass extracts. Soil Sci. Soc. Am. J. 57, 1007–1012. https://doi.org/10.2136/sssaj1993.03615995005700040021x.

Chen, D.M., Lan, Z.C., Hu, S.J., Bai, Y.F., 2015. Effects of nitrogen enrichment on belowground communities in grassland: Relative role of soil nitrogen availability vs. soil acidification. Soil Biol. Biochem. 89, 99–108. https://doi.org/10.1016/j.soilbio.2015.06.028.

Cheng, L., Zhang, N.F., Yuan, M.T., Xiao, J., Qin, Y.J., Deng, Y., Tu, Q.C., Xue, K., Van Nostrand, J.D., Wu, L.Y., He, Z.L., Zhou, X.H., Leigh, M.B., Konstantinidis, K.T., Schuur, E.A., Luo, Y.Q., Tiedje, J.M., Zhou, J.Z., 2017. Warming enhances old organic carbon decomposition through altering functional microbial communities. ISME J. 11, 1825–1835. https://doi.org/10.1038/ismej.2017.48.

Edwards, I.P., Zak, D.R., Kellner, H., Eisenlord, S.D., Pregitzer, K.S., 2011. Simulated atmospheric N deposition alters fungal community composition and suppresses ligninolytic gene expression in a northern hardwood forest. PLoS One 6, e20421. https://doi.org/10.1371/journal.pone.0020421.

Eisenlord, S.D., Freedman, Z., Zak, D.R., Xue, K., He, Z.L., Zhou, J.Z., 2013. Microbial mechanisms mediating increased soil C storage under elevated atmospheric N deposition. Appl. Environ. Microb. 79, 1191–1199. https://doi.org/10.1128/AEM.03156-12.

Falkowski, P.G., Fenchel, T., Delong, E.F., 2008. The microbial engines that drive Earth's biogeochemical cycles. Science 320, 1034–1039. https://doi.org/10.1126/science.1153213.

Fierer, N., Lauber, C.L., Ramirez, K.S., Zaneveld, J., Bradford, M.A., Knight, R., 2012. Comparative metagenomic, phylogenetic and physiological analyses of soil microbial communities across nitrogen gradients. ISME J. 6, 1007–1017. https://doi.org/10.1038/ismej.2011.159.

Freedman, Z., Eisenlord, S.D., Zak, D.R., Xue, K., He, Z.L., Zhou, J.Z., 2013. Towards a molecular understanding of N cycling in northern hardwood forests under future rates of N deposition. Soil Biol. Biochem. 66, 130–138. https://doi.org/10.1016/j.soilbio.2013.07.010.

Garcia-Palacios, P., Shaw, E.A., Wall, D.H., Hattenschwiler, S., 2016. Temporal dynamics of biotic and abiotic drivers of litter decomposition. Ecol. Lett. 19, 554–563. https://doi.org/10.1111/ele.12590.

German, D.P., Weintraub, M.N., Grandy, A.S., Lauber, C.L., Rinkes, Z.L., Allison, S.D., 2011. Optimization of hydrolytic and oxidative enzyme methods for ecosystem studies. Soil Biol. Biochem. 43, 1387–1397. https://doi.org/10.1016/j.soilbio.2011.03.017.

Guo, P., Jia, J.L., Han, T.W., Xie, J.X., Wu, P.F., Du, Y.H., Qu, K.Y., 2017. Nonlinear responses of forest soil microbial communities and activities after short- and long-term gradient nitrogen additions. Appl. Soil Ecol. 121, 60–64. https://doi.org/10.1016/j.apsoil.2017.09.018.

Huang, J.X., Lin, T.C., Xiong, D.C., Yang, Z.J., Liu, X.F., Chen, G.S., Xie, J.S., Li, Y.Q., Yang, Y.S., 2019. Organic carbon mineralization in soils of a natural forest and a forest plantation of southeastern China. Geoderma 344, 119–126. https://doi.org/10.1016/j.geoderma.2019.03.012.

Jing, H., Zhang, P., Li, J.J., Yao, X., Liu, G.B., Wang, G.L., 2019. Effect of nitrogen addition on the decomposition and release of compounds from fine roots with different diameters: the importance of initial substrate chemistry. Plant Soil 438, 281–296. https://doi.org/10.1007/s11104-019-04017-w.

Joergensen, R.G., 1996. The fumigation-extraction method to estimate soil microbial biomass: Calibration of the k_{EC} value. Soil Biol. Biochem. 28, 25–31. https://doi.org/10.1016/0038-0717(95)00101-8.

Levy-Booth, D.J., Prescott, C.E., Grayston, S.J., 2014. Microbial functional genes involved in nitrogen fixation, nitrification and denitrification in forest ecosystems. Soil Biol. Biochem. 75, 11–25. https://doi.org/10.1016/j.soilbio.2014.03.021.

Li, H., Yang, S., Xu, Z., Yan, Q., Li, X., van Nostrand, J.D., He, Z., Yao, F., Han, X., Zhou, J.J.S.B., 2017. Responses of soil microbial functional genes to global changes are indirectly influenced by aboveground plant biomass variation. Biochemistry. 104, 18–29. https://doi.org/10.1016/j.soilbio.2016.10.009.

Li, J.J., Wang, G.L., Yan, B.S., Liu, G.B., 2020. The responses of soil nitrogen transformation to nitrogen addition are mainly related to the changes in functional gene relative abundance in artificial Pinus tabulaeformis forests. Sci. Total Environ. 723, 137679.

Li, P., Shen, C.C., Jiang, L., Feng, Z.Z., Fang, J.Y., 2019. Difference in soil bacterial community composition depends on forest type rather than nitrogen and phosphorus additions in tropical montane rainforests. Biol. Fertil. Soils 55, 313–323. https://doi.org/10.1007/s00374-019-01349-8.

Liu, W.X., Jiang, L., Hu, S.J., Li, L.H., Liu, L.L., Wan, S.Q., 2014. Decoupling of soil microbes and plants with increasing anthropogenic nitrogen inputs in a temperate steppe. Soil Biol. Biochem. 72, 116–122. https://doi.org/10.1016/j.soilbio.2014.01.022.

Liu, Y., Liu, G., Xiong, Z., Liu, W., 2017. Response of greenhouse gas emissions from three types of wetland soils to simulated temperature change on the Qinghai-Tibetan Plateau. Atmos. Environ. 171, 17–24. https://doi.org/10.1016/j.atmosenv.2017.10.005.

Lv, F.L., Xue, S., Wang, G.L., Zhang, C., 2017. Nitrogen addition shifts the microbial community in the rhizosphere of Pinus tabuliformis in Northwestern China. PLoS One 12, e0172382. https://doi.org/10.1371/journal.pone.0172382.

Magnani, F., Mencuccini, M., Borghetti, M., Berbigier, P., Berninger, F., Delzon, S., Grelle, A., Hari, P., Jarvis, P.G., Kolari, P., Kowalski, A.S., Lankreijer, H., Law, B.E., Lindroth, A., Loustau, D., Manca, G., Moncrieff, J.B., Rayment, M., Tedeschi, V., Valentini, R., Grace, J., 2007. The human footprint in the carbon cycle of temperate and boreal forests. Nature 447, 848–850. https://doi.org/10.1038/nature05847.

Mao, Q.G., Lu, X.K., Zhou, K.J., Chen, H., Zhu, X.M., Mori, T.K., Mo, J.M., 2017. Effects of long-term nitrogen and phosphorus additions on soil acidification in an N-rich tropical forest. Geoderma 285, 57–63. https://doi.org/10.1016/j.geoderma.2016.09.017.

Marx, M.C., Wood, M., Jarvis, S.C., 2001. A microplate fluorimetric assay for the study of enzyme diversity in soils. Soil Biol. Biochem. 33, 1633–1640. https://doi.org/10.1016/S0038-0717(01)00079-7.

Nannipieri, P., Penton, C.R., Purahong, W., Schloter, M., van Elsas, J.D., 2019. Recommendations for soil microbiome analyses. Biol. Fertil. Soils 55, 765–766. https://doi.org/10.1007/s00374-019-01409-z.

Norby, R.J., Ledford, J., Reilly, C.D., Miller, N.E., O'Neill, E.G., 2004. Fine-root production dominates response of a deciduous forest to atmospheric CO_2 enrichment. P. Natl. Acad. Sci. USA 101, 9689–9693. https://doi.org/10.1073/pnas.0403491101.

Olsen, S.R., Sommers, L.E., 1982. Phosphorous. In: Page, A.L., Miller, R.H., Keeney, D.R. (Eds.), Methods of Soil Analysis. Chemical and Microbial Properties. Agronomy Society of America, Madison, pp. 403–430.

Riggs, C.E., Hobbie, S.E., 2016. Mechanisms driving the soil organic matter decomposition response to nitrogen enrichment in grassland soils. Soil Biol. Biochem. 99, 54–65. https://doi.org/10.1016/j.soilbio.2016.04.023.

Riggs, C.E., Hobbie, S.E., Bach, E.M., Hofmockel, K.S., Kazanski, C.E., 2015. Nitrogen addition changes grassland soil organic matter decomposition. Biogeochemistry 125, 203–219. https://doi.org/10.1007/s10533-015-0123-2.

Rocca, J.D., Hall, E.K., Lennon, J.T., Evans, S.E., Waldrop, M.P., Cotner, J.B., Nemergut, D.R., Graham, E.B., Wallenstein, M.D., 2015. Relationships between protein-encoding gene abundance and corresponding process are commonly assumed yet rarely observed. ISME J. 9, 1693–1699. https://doi.org/10.1038/ismej.2014.252.

Sun, L.P., Jing, H., Wang, G.L., Liu, G.B., 2018. Nitrogen addition increases the contents of glomalin-related soil protein and soil organic carbon but retains aggregate stability in a *Pinus tabulaeformis* forest. Peerj 6. https://doi.org/10.7717/peerj.5039.

Treseder, K.K., 2004. A meta-analysis of mycorrhizal responses to nitrogen, phosphorus, and atmospheric CO_2 in field studies. New Phytol. 164, 347–355. https://doi.org/10.1111/j.1469-8137.2004.01159.x.

Treseder, K.K., 2008. Nitrogen additions and microbial biomass: a meta-analysis of ecosystem studies. Ecol. Lett. 11, 1111–1120. https://doi.org/10.1111/j.1461-0248.2008.01230.x.

Trivedi, P., Delgado-Baquerizo, M., Trivedi, C., Hu, H.W., Anderson, I.C., Jeffries, T.C., Zhou, J.Z., Singh, B.K., 2016. Microbial regulation of the soil carbon cycle: evidence from gene-enzyme relationships. ISME J. 10, 2593–2604. https://doi.org/10.1038/ismej.2016.65.

Vance, E.D., Brookes, P.C., Jenkinson, D.S., 1987. An extraction method for measuring soil microbial biomass C. Soil Biol. Biochem. 19, 703–707. https://doi.org/10.1016/0038-0717(87)90052-6.

Wang, C., Lu, X., Mori, T., Mao, Q., Zhou, K., Zhou, G., Nie, Y., Mo, J.J.S.B., 2018a. Responses of soil microbial community to continuous experimental nitrogen additions for 13 years in a nitrogen-rich tropical forest. Soil Biol. Biochem. 121, 103–112. https://doi.org/10.1016/j.soilbio.2018.03.009.

Wang, H., Liu, S.R., Zhang, X., Mao, Q.G., Li, X.Z., You, Y.M., Wang, J.X., Zheng, M.H., Zhang, W., Lu, X.K., Mo, J.M., 2018b. Nitrogen addition reduces soil bacterial richness, while phosphorus addition alters community composition in an old-growth N-rich tropical forest in southern China. Soil Biol. Biochem. 127, 22–30. https://doi.org/10.1016/j.soilbio.2018.08.022.

Wang, J., Liu, G.B., Zhang, C., Wang, G.L., Fang, L.C., Cui, Y.X., 2019a. Higher temporal turnover of soil fungi than bacteria during long-term secondary succession in a semiarid abandoned farmland. Soil Till. Res. 194, 104305 https://doi.org/10.1016/j.still.2019.104305.

Wang, M.M., Wang, S.P., Wu, L.W., Xu, D.P., Lin, Q.Y., Hu, Y.G., Li, X.Z., Zhou, J.Z., Yang, Y.F., 2016a. Evaluating the lingering effect of livestock grazing on functional potentials of microbial communities in Tibetan grassland soils. Plant Soil 407, 385–399. https://doi.org/10.1007/s11104-016-2897-y.

Wang, R.Z., Dorodnikov, M., Dijkstra, F.A., Yang, S., Xu, Z.W., Li, H., Jiang, Y., 2016b. Sensitivities to nitrogen and water addition vary among microbial groups within soil aggregates in a semiarid grassland. Biol. Fertil. Soils 53, 129–140. https://doi.org/10.1007/s00374-016-1165-x.

Wang, W.J., Mo, Q.F., Han, X.G., Hui, D.F., Shen, W.J., 2019b. Fine root dynamics responses to nitrogen addition depend on root order, soil layer, and experimental duration in a subtropical forest. Biol. Fertil. Soils 55, 723–736. https://doi.org/10.1007/s00374-019-01386-3.

Wang, Y.S., Cheng, S.L., Fang, H.J., Yu, G.R., Xu, X.F., Xu, M.J., Wang, L., Li, X.Y., Si, G.Y., Geng, J., He, S., 2015. Contrasting effects of ammonium and nitrate inputs on soil CO_2 emission in a subtropical coniferous plantation of southern China. Biol. Fertil. Soils 51, 815–825. https://doi.org/10.1007/s00374-015-1028-x.

Wei, W., Yang, M., Liu, Y.X., Huang, H.C., Ye, C., Zheng, J.F., Guo, C.W., Hao, M.W., He, X.H., Zhu, S.S., 2018. Fertilizer N application rate impacts plant-soil feedback in a sanqi production system. Sci. Total Environ. 633, 796–807. https://doi.org/10.1016/j.scitotenv.2018.03.219.

Wei, Y., Tong, Y.A., Qiao, L., Liu, X.J., Duan, M., Li, J., 2010. Preliminary estimation of the atmosphere nitrogen deposition in different ecological regions of Shaanxi province. J. Agro-Environ. Sci. 29, 795–800.

Wood, S.A., Bradford, M.A., Gilbert, J.A., McGuire, K.L., Palm, C.A., Tully, K.L., Zhou, J.Z., Naeem, S., 2015. Agricultural intensification and the functional capacity of soil microbes on smallholder African farms. J. Appl. Ecol. 52, 744–752. https://doi.org/10.1111/1365-2664.12416.

Xiao, L., Liu, G.B., Li, P., Xue, S., 2019. Direct and indirect effects of elevated CO_2 and nitrogen addition on soil microbial communities in the rhizosphere of Bothriochloa ischaemum. J. Soils Sediment 19, 3679–3687. https://doi.org/10.1007/s11368-019-02336-0.

Xu, W.F., Yuan, W.P., Cui, L.L., Ma, M.N., Zhang, F.G., 2019. Responses of soil organic carbon decomposition to warming depend on the natural warming gradient. Geoderma 343, 10–18. https://doi.org/10.1016/j.geoderma.2019.02.017.

Yao, X., Jing, H., Liang, C.T., Gu, L.C., Wang, G.L., Xue, S., 2017. Response of labile organic carbon content in surface soil aggregates to short-term nitrogen addition in artificial *Pinus tabulaeformis* forests. Acta Ecological Sinica 37, 6724–6731. https://doi.org/10.5846/stxb201608021590.

Zeng, J., Liu, X.J., Song, L., Lin, X.G., Zhang, H.Y., Shen, C.C., Chu, H.Y., 2016. Nitrogen fertilization directly affects soil bacterial diversity and indirectly affects bacterial community composition. Soil Biol. Biochem. 92, 41–49. https://doi.org/10.1016/j.soilbio.2015.09.018.

Zhang, J.Y., Ai, Z.M., Liang, C.T., Wang, G.L., Xue, S., 2017a. Response of soil microbial communities and nitrogen thresholds of Bothriochloa ischaemum to short-term nitrogen addition on the Loess Plateau. Geoderma 308, 112–119. https://doi.org/10.1016/j.geoderma.2017.08.034.

Zhang, Y.G., Liu, X., Cong, J., Lu, H., Sheng, Y.Y., Wang, X.L., Li, D.Q., Liu, X.D., Yin, H.Q., Zhou, J.Z., Deng, Y., 2017b. The microbially mediated soil organic carbon loss under degenerative succession in an alpine meadow. Mol. Ecol. 26, 3676–3686. https://doi.org/10.1111/mec.14148.

Zhong, Y.Q.W., Yan, W.M., Wang, R.W., Wang, W., Shangguan, Z.P., 2018. Decreased occurrence of carbon cycle functions in microbial communities along with long-term secondary succession. Soil Biol. Biochem. 123, 207–217. https://doi.org/10.1016/j.soilbio.2018.05.017.

Zhou, J.Z., Xue, K., Xie, J.P., Deng, Y., Wu, L.Y., Cheng, X.L., Fei, S.F., Deng, S.P., He, Z.L., Van Nostrand, J.D., Luo, Y.Q., 2011. Microbial mediation of carbon-cycle feedbacks to climate warming. Nat. Clim. Change 2, 106–110. https://doi.org/10.1038/nclimate1331.

Zhou, L.Y., Zhou, X.H., Zhang, B.C., Lu, M., Luo, Y.Q., Liu, L.L., Li, B., 2014. Different responses of soil respiration and its components to nitrogen addition among biomes: a meta-analysis. Global Chang Biol. 20, 2332–2343. https://doi.org/10.1111/gcb.12490.

Zhou, Z.H., Wang, C.K., Zheng, M.H., Jiang, L.F., Luo, Y.Q., 2017. Patterns and mechanisms of responses by soil microbial communities to nitrogen addition. Soil Biol. Biochem. 115, 433–441. https://doi.org/10.1016/j.soilbio.2017.09.015.

Zhu, C., Ma, Y.P., Wu, H.H., Sun, T., La Pierre, K.J., Sun, Z.W., Yu, Q., 2016. Divergent Effects of Nitrogen Addition on Soil Respiration in a Semiarid Grassland. Sci. Rep. 6, 33541. https://doi.org/10.1038/srep33541.

Zhu, Z., Ge, T., Liu, S., Hu, Y., Ye, R., Xiao, M., Tong, C., Kuzyakov, Y., Wu, J., 2018. Rice rhizodeposits affect organic matter priming in paddy soil: The role of N fertilization and plant growth for enzyme activities, CO_2 and CH_4 emissions. Soil Biology and Biochemistry 116, 369–377. https://doi.org/10.1016/j.soilbio.2017.11.001.